Supporting Information for:

A Multicolor Photochromic Gel Based on Temporal Separation of Photochemical Reactions

Yuki Nakai,‡[a] Yuki Nagai,‡*[a] Yukihiro Furukawa,[a] Yoichi Kobayashi*[a]

a) Department of Applied Chemistry, College of Life Sciences, Ritsumeikan University, 1-1-1 Nojihigashi, Kusatsu, Shiga 525-8577, Japan.

‡ These authors contributed equally to this work.

E-mail: ynagai@fc.ritsumei.ac.jp; ykobayas@fc.ritsumei.ac.jp

Contents

General methods

Materials

Anthraquinone (AQ), 1,2-bis(2,4-dimethyl-5-phenyl-3-thienyl)-3,3,4,4,5,5-hexafluoro-1-cyclopentene (DE), boc-L-glutamic acid, and 1-hydroxybenzotrizole were purchased from Tokyo Chemical Industry Co. (TCI). Octadecylamine and 1-ethyl-3-(3-dimethylaminopropyl)carbodiimide hydrochloride, triethylamine (TEA), sodium hydroxide (NaOH), and ethanol (EtOH, for spectrochemical analysis) were purchased from FUJIFILM Wako Pure Chemical Co. Dichloromethane, tetrahydrofuran, and chloroform-d were purchased from Kanto Chemical Co. All chemicals were used without further purification.

Sample preparation:

Typically, anthraquinone (AQ, 2.8×10^{-4} M, 7×10^{-3} wt%), the diarylethene derivative (DE, 2.9×10^{-4} M, 2.0×10^{-2} wt%), triethylamine (TEA, 1.9×10^{-3} M, 2.4×10^{-2} wt%), and sodium hydroxide (NaOH, 6×10^{-3} M, 3.0×10^{-2} wt%) were dissolved in EtOH to give the solution samples. For the gel sample, LBG (9×10^{-3} M, 8.5×10^{-1} wt%) was added to the solution and dissolved by heating to 50 °C. The obtained sol was left at room temperature to give the gel. Bubbling for the gel sample was conducted in the sol state.

For recording sample images, AQ-DE gels were prepared by changing the concentrations as follows: AQ 8.5×10^{-4} M (1.7×10^{-2} wt%), DE 8.6×10^{-4} M (4.5×10^{-2} wt%), TEA 5.7×10^{-3} M (5.4×10^{-2} wt%), NaOH 1.8×10^{-2} M (5.4×10^{-2} wt%), LBG 1.3×10^{-2} M (1.2 wt%). This is because the typical concentration condition was optimized for spectroscopy. In the typical condition, the color changes were obvious in naked-eye observations but unclear in images.

Photoinduced coloration and decoloration:

Ultraviolet (UV) light irradiation was conducted using an LED power source (UPS0350D10, DAICO MFG) and a 340-nm LED head (DSL-340S, DAICO MFG) equipped with a rod lens (RLQL80-1, Asahi Spectra). The UV light intensity was set to ~0.15 mW except for the light intensity dependence measurement (Fig. S5b) and the sample image recording (0.4 mW cm^{-2} for Fig. 3a and Fig. 4, 0.2 mW cm^{-2} for Fig. 5). Visible (Vis) light irradiation was conducted using an LED power source (CL-1501, Asahi Spectra) and a 525-nm LED head (CL-H1-525-7-1-B, Asahi Spectra). The Vis light intensity was set to 15 mW cm^{-2} except for the sample image recording (38 mW cm^{-2} for Fig. 3a and Fig. 4, 33 mW cm^{-2} for Fig. 5). The LED powers were measured by a power meter (PD300RM-UV, Ophir)

Air-oxidation of the reduced form of AQ was conducted by shaking the cuvette in the sol state heated up to 50 °C.

UV-Vis-near-infrared (NIR) absorption spectroscopy:

UV-Vis-NIR spectra were measured on a UV-3600 spectrometer (SHIMADZU). The 1-mm quartz cuvette was used.

Measurements of the time evolution of absorption:

Absorbance changes over time were traced using a multichannel spectrometer (OCEAN FX, Ocean Optics) as a detector and a deuterium-halogen light source (DH-2000-BAL, Ocean Optics) as a probe light source. To suppress

photochemical reactions induced by the probe light and effects of the excitation light on absorption spectra, light sources were controlled by a home-made MATLAB code in the following ways. For measurements of coloration dynamics under 340-nm light, the probe light was irradiated for only 0.1 s per 2.1 s, respectively, except for the light intensity dependence measurements (Fig. S5b). For the light intensity dependence measurements, the probe light was irradiated for only 0.1 s per X s, respectively; X was tuned from 2.1 to 6.4, depending on the excitation light intensity. The spectral data were acquired during the probe light irradiation. For measurements of decoloration dynamics induced by 525-nm light, the probe light and the 525-nm LED light were alternatingly irradiated for 0.1 s and 2.0 s, respectively. The spectral data were acquired during the probe light irradiation. The 1-mm quartz cuvette was used.

Gas composition control:

Two gas flowmeters (NFM-V-P-A-500-C, TEHKNE Corporation) were connected to the nitrogen gas line and a diaphragm pump discharging the air, respectively. The flow-regulated nitrogen and air were mixed using a T-shaped tube, and the mixed gas was used for the bubbling operation. The volume fraction of oxygen in the mixed gas was calculated, assuming the oxygen volume fraction in the air is 0.21.

Multicolor photopatterning:

The photomask was fabricated by combining aluminum foil and polyester film (Fig. S10). The transmittance of each part of the photomask was determined from the 340-nm LED intensities measured by a UV-3600 spectrometer (SHIMADZU). The gel sample was prepared in a 1-mm quartz cuvette.

Synthesis

Synthesis of LBG (*N*,*N*'-bis(octadecyl)-L-Boc-glutamic diamide)

LBG was synthesized according to the literature.[1] Boc-L-glutamic acid (309.8 mg, 1.02 mmol) and octadecyl amine (960.2 mg, 3.56 mmol) were added to dichloromethane (30 mL). 1-Ethyl-3-(3-dimethlaminopropyl)carbodiimide hydrochloride (528.1 mg, 2.75 mmol) and 1-hydroxybenzotrizole (500.8 mg, 3.27 mmol) were added to the mixture, followed by stirring at room temperature for 72 hours. The obtained colorless solid was collected by filtration. The crude product was dissolved in tetrahydrofuran and reprecipitated by the addition of water twice. Drying the precipitates under vacuum gave a colorless solid (0.56 g, 74% yield).

^{1}H-NMR (Chloroform-d/TMS, 500 MHz): δ 6.57 (s, 1H), δ 5.97 (s, 1H), δ 5.70 (s, 1H), δ 4.07 (m, 1H), δ 3.24 (m, 4H), δ 2.29 (m, 2H), δ 1.90–2.06 (m, 2H), δ 1.48–1.52 (m, 4H), δ 1.43 (s, 9H), δ 1.25 (br s, 60H), δ 0.88 (t, J = 6.4 Hz, 6H).

The NMR peak positions were consistent with the literature.[1]

Absorption spectra of the DE-AQ gel at each state

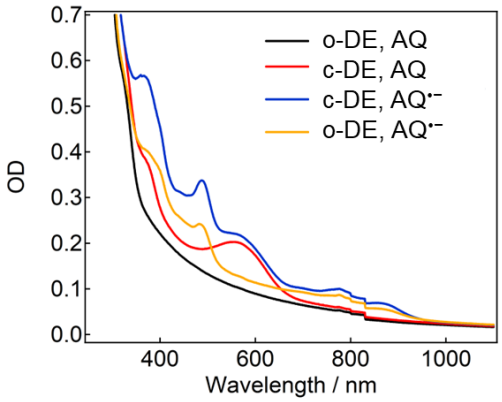

Fig. S1 Absorption spectra of the DE-AQ gel (2.8×10^{-4} M DE, 2.9×10^{-4} M AQ, 1.9×10^{-3} M TEA, 6×10^{-3} M NaOH in air-saturated EtOH, 1-mm cuvette). Each state was achieved by combining 340 and 525 nm-light irradiations and the sol–gel transition.

Coloration dynamics of DE

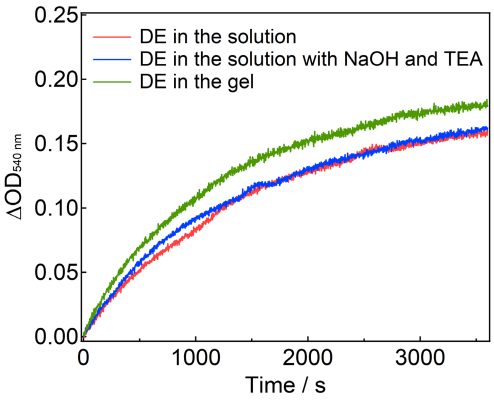

Fig. S2 Coloration dynamics at 540 nm of DE (2.8×10^{-4} M, in the 1-mm cuvette) under 340-nm light irradiation (0.13 mW cm^{-2}) in (red) EtOH, (blue) EtOH containing 1.9×10^{-3} M TEA and 6×10^{-3} M NaOH, and (green) the LBG EtOH gel (1×10^{-2} M).

In all samples, the coloration dynamics were not so different from that of the DE-AQ gel. These results show that TEA, NaOH, LBG, and AQ had little influence on the photoconversion of DE.

The coloration of the closed form of DE (c-DE) was much weaker than that in a previous study.[2] A major reason for this is the difference in the excitation wavelength. DE was excited at 313 nm in the previous study, but it was excited at 340 nm in this study, considering the balance of absorption coefficients of DE and AQ. Unfortunately, c-DE shows much stronger absorption at 340 nm than at 313 nm, lowering the conversion ratio. Additionally, AQ also absorbs the excitation light, slowing down the photoconversion from open-DE (o-DE) to c-DE.

Absorption spectral change under 525-nm light irradiation

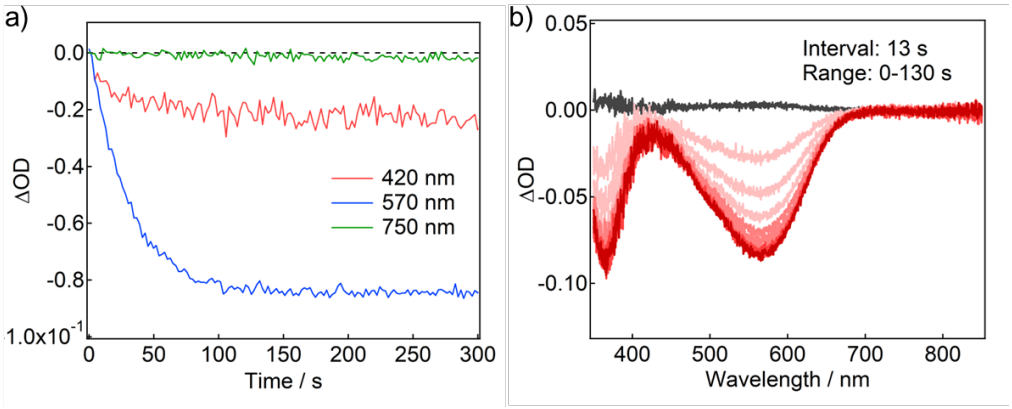

Fig. S3 (a) Absorption change dynamics at 420, 570, and 750 nm and (b) absorption spectral changes of the DE-AQ gel (2.8×10^{-4} M DE, 2.9×10^{-4} M AQ, 1.9×10^{-3} M TEA, 6×10^{-3} M NaOH in air-saturated EtOH, 1-mm cuvette) under 525-nm light irradiation (15 mW cm^{-2}).

Cyclability of multicolor photochromism

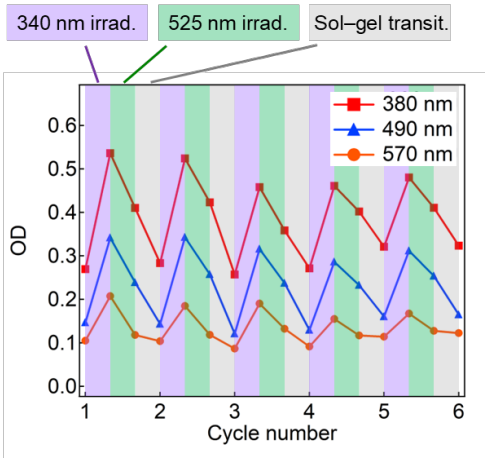

Fig. S4 Cyclability of multicolor photochromism in the DE-AQ gel (2.8×10^{-4} M DE, 2.9×10^{-4} M AQ, 1.9×10^{-3} M TEA, 6×10^{-3} M NaOH in air-saturated EtOH, 1-mm cuvette). 340-nm light irradiation: 0.13 mW cm^{-2}, 60 min; 525-nm light irradiation: 15 mW cm^{-2}, 5 min.

Dependence of the temporal separation degree on the gas composition and light intensity

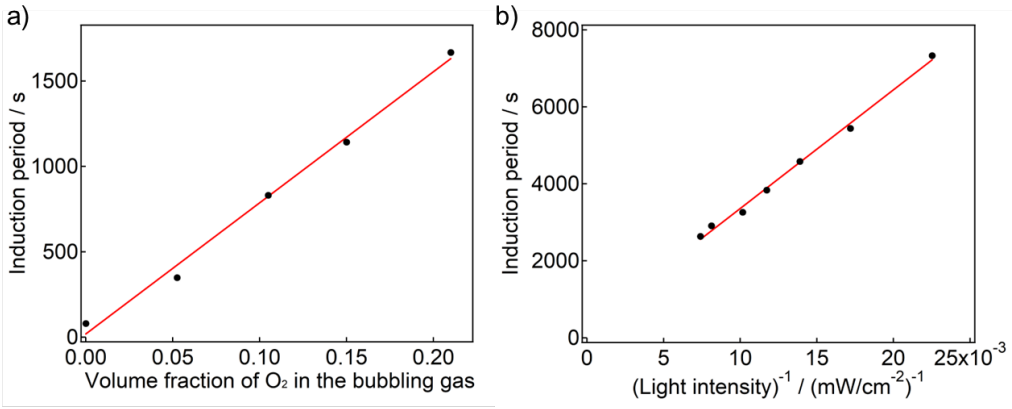

Fig. S5 (a,b) The induction periods of the AQ photoreduction in the DE-AQ gel (2.8×10^{-4} M DE, 2.9×10^{-4} M AQ, 1.9×10^{-3} M TEA, 6×10^{-3} M NaOH in EtOH, 1-mm cuvette) under 340-nm light irradiation; (a) vs. the bubbling gas composition (340-nm light: 0.13 mW cm^{-2}), (b) vs. 340-nm light intensity (in the air-saturated gel). The volume fraction of oxygen in the mixed gas was calculated, assuming the oxygen volume fraction in the air is 0.21.

Multicolor photochromism under intense excitation light

In this work, we combined a rod lens with the 340-nm LED light to make homogeneous photoirradiation, because our solid-like gel samples could not be stirred. Unfortunately, the rod lens significantly weakened the LED light intensity, leading to the slow photochromic reaction in our samples. When we did not use the rod lens (The excitation intensity around the probe area: ~19 mW cm^{-2}), the two-step coloration was completed within a minute.

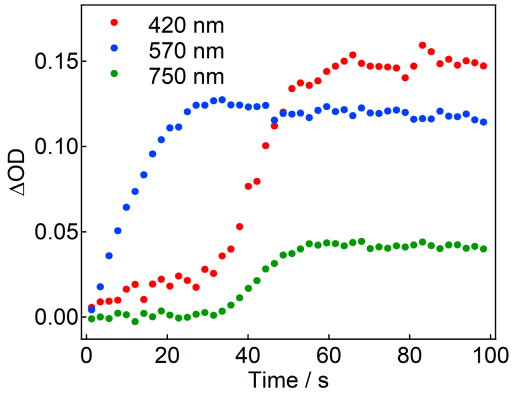

Fig. S6 Absorption change dynamics at 420, 570, and 750 nm of the DE-AQ gel (2.8×10^{-4} M DE, 2.9×10^{-4} M AQ, 1.9×10^{-3} M TEA, 6×10^{-3} M NaOH in air-saturated EtOH, 1-mm cuvette) under 340-nm light irradiation (~19 mW cm^{-2}, the rod lens was not used for this experiment).

Dependence of the AQ concentration and the cuvette thickness

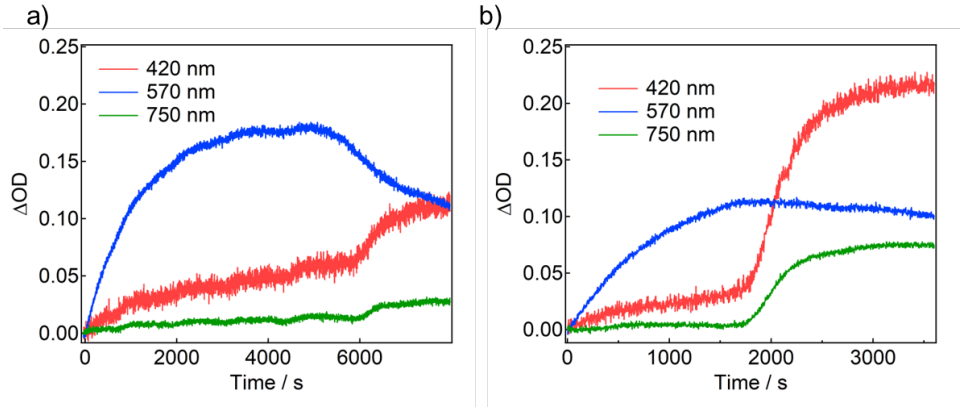

Fig. S7 Absorption change dynamics at 420, 570, and 750 nm of the DE-AQ gel (2.8×10^{-4} M DE, 1.9×10^{-3} M TEA, 6×10^{-3} M NaOH in air-saturated EtOH, 1-mm cuvette) under 340-nm light irradiation (0.13 mW cm^{-2}). The AQ concentration: (a) 1.1×10^{-4} M, (b) 4.5×10^{-4} M.

The induction period was shorter as the AQ concentration was higher, because the oxygen consumption triggered by the excitation of AQ was promoted. Notably, the decomposition of c-DE after the induction period was more significant in the case of lower AQ concentration. This result suggests that the excitation of c-DE with UV light in the presence of $AQ^{\bullet-}$ caused the decomposition of c-DE. In the case that the AQ concentration was higher, more $AQ^{\bullet-}$ was produced, suppressing the excitation and probably thereby the photodecomposition of c-DE. In contrast, in the case that the AQ concentration was lower, c-DE absorbed more photons, leading to more photodecomposition.

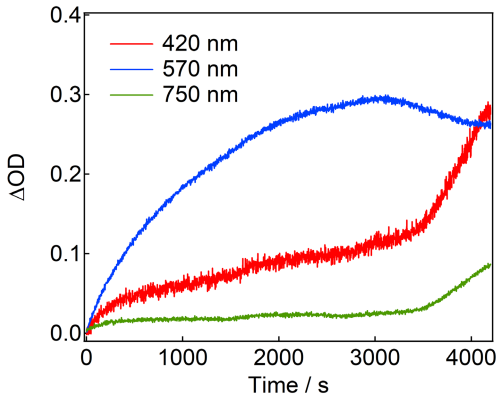

Fig. S8 Absorption change dynamics at 420, 570, and 750 nm of the DE-AQ gel (2.8×10^{-4} M DE, 2.9×10^{-4} M AQ, 1.9×10^{-3} M TEA, 6×10^{-3} M NaOH in air-saturated EtOH, 2-mm cuvette) under 340-nm light irradiation (0.13 mW cm^{-2}).

In the 2-mm cuvette, absorption changes were almost doubled compared to the case of the 1-mm cuvette. The induction period was also slightly longer than in the 1-mm cuvette, probably because the thickness prevented the excitation light from penetrating the inside of the sample.

Simulation of the reaction kinetics until the photoreduction of AQ

Here, the reaction kinetics until the beginning of photoreduction of AQ are theoretically simulated using a simple reaction model. Absorbance of the sample A_{tot} (the scattering is ignored) is given the following equation:

$$\begin{aligned} A_{\mathrm{tot}} &= A_{\text{o-DE}} + A_{\text{c-DE}} + A_{\mathrm{AQ}} \\ &= \varepsilon_{\text{o-DE}} \cdot C_{\text{o-DE}} \cdot l + \varepsilon_{\text{c-DE}} \cdot C_{\text{c-DE}} \cdot l + \varepsilon_{\mathrm{AQ}} \cdot C_{\mathrm{AQ}} \cdot l \\ &= (\varepsilon_{\text{o-DE}} \cdot C_{\text{o-DE}} + \varepsilon_{\text{c-DE}} \cdot C_{\text{c-DE}} + \varepsilon_{\mathrm{AQ}} \cdot C_{\mathrm{AQ}}) \cdot l \\ &= a_{\mathrm{tot}} \cdot l \end{aligned}$$

$$(a_{\mathrm{tot}} = \varepsilon_{\text{o-DE}} \cdot C_{\text{o-DE}} + \varepsilon_{\text{c-DE}} \cdot C_{\text{c-DE}} + \varepsilon_{\mathrm{AQ}} \cdot C_{\mathrm{AQ}})$$

where A_{x}, ε_{x}, C_{x}, and l denote the absorbance and the molar absorption coefficient [$\mathrm{cm^{-1}\ M^{-1}}$] at the irradiated light wavelength and the concentration [M] of each component, the optical path length [cm]. The numbers of photons absorbed by o-DE, c-DE, and AQ per second $I_{\text{o-DE}}$, $I_{\text{c-DE}}$, and I_{AQ} [$\mathrm{mol\ s^{-1}}$] are given by the following equations, respectively:

$$I_{\text{o-DE}} = I \cdot (1 - 10^{-A_{\mathrm{tot}}}) \cdot \frac{A_{\text{o-DE}}}{A_{\mathrm{tot}}} = I \cdot (1 - 10^{-a_{\mathrm{tot}} \cdot l}) \cdot \frac{\varepsilon_{\text{o-DE}} \cdot C_{\text{o-DE}}}{a_{\mathrm{tot}}}$$

$$I_{\text{c-DE}} = I \cdot (1 - 10^{-a_{\mathrm{tot}} \cdot l}) \cdot \frac{\varepsilon_{\text{c-DE}} \cdot C_{\text{c-DE}}}{a_{\mathrm{tot}}}$$

$$I_{\mathrm{AQ}} = I \cdot (1 - 10^{-a_{\mathrm{tot}} \cdot l}) \cdot \frac{\varepsilon_{\mathrm{AQ}} \cdot C_{\mathrm{AQ}}}{a_{\mathrm{tot}}}$$

The cumulative number of photons absorbed by AQ per area, N_{AQ} [$\mathrm{mol\ cm^{-2}}$] at an arbitrary time is denoted by the following equation, if C_{AQ} is constant until then:

$$N_{\mathrm{AQ}} = \int_0^t I_{\mathrm{AQ}}\,\mathrm{d}t = \varepsilon_{\mathrm{AQ}} \cdot C_{\mathrm{AQ}} \cdot I \cdot \int_0^t \frac{1 - 10^{-a_{\mathrm{tot}} \cdot l}}{a_{\mathrm{tot}}}\,\mathrm{d}t$$

The time derivatives of $C_{\text{o-DE}}$ and $C_{\text{c-DE}}$ were given by the following equations:

$$\begin{aligned} \frac{\mathrm{d}C_{\text{o-DE}}}{\mathrm{d}t} &= -I_{\text{o-DE}} \cdot \varphi_{\text{o}\to\text{c}} + I_{\text{cDE}} \cdot \varphi_{\text{c}\to\text{o}} \\ &= \frac{I \cdot (1 - 10^{-a_{\mathrm{tot}} \cdot l})}{a_{\mathrm{tot}}} \cdot (-\varepsilon_{\text{o-DE}} \cdot C_{\text{o-DE}} \cdot \varphi_{\text{o}\to\text{c}} + \varepsilon_{\text{c-DE}} \cdot C_{\text{c-DE}} \cdot \varphi_{\text{c}\to\text{o}}) \\ &= \frac{I \cdot (1 - 10^{-a_{\mathrm{tot}} \cdot l})}{a_{\mathrm{tot}}} \cdot \{-\varepsilon_{\text{o-DE}} \cdot C_{\text{o-DE}} \cdot \varphi_{\text{o}\to\text{c}} + \varepsilon_{\text{c-DE}} \cdot (C_{\mathrm{DE}} - C_{\text{o-DE}}) \cdot \varphi_{\text{c}\to\text{o}}\} \end{aligned}$$

$$\begin{aligned} \frac{\mathrm{d}C_{\text{c-DE}}}{\mathrm{d}t} &= I_{\text{o-DE}} \cdot \varphi_{\text{o}\to\text{c}} - I_{\text{c-DE}} \cdot \varphi_{\text{c}\to\text{o}} \\ &= \frac{I \cdot (1 - 10^{-a_{\mathrm{tot}} \cdot l})}{a_{\mathrm{tot}}} \cdot \{\varepsilon_{\text{o-DE}} \cdot (C_{\mathrm{DE}} - C_{\text{c-DE}}) \cdot \varphi_{\text{o}\to\text{c}} - \varepsilon_{\text{c-DE}} \cdot C_{\text{c-DE}} \cdot \varphi_{\text{c}\to\text{o}}\} \end{aligned}$$

$$(C_{\mathrm{DE}} = C_{\text{o-DE}} + C_{\text{c-DE}})$$

where $\varphi_{\text{o}\to\text{c}}$ and $\varphi_{\text{c}\to\text{o}}$ denote the quantum yields in the ring closing reaction from o-DE to c-DE and the ring opening reaction from c-DE to o-DE, respectively.

The solver ode45 in Matlab solved the above differential equations using the below initial values, to give the time courses of $C_{\text{o-DE}}$, $C_{\text{c-DE}}$, and N_{AQ} (Fig. S9). N_{AQ} showed an almost linear relationship vs time (Fig. S9b).

$C_{\text{o-DE}} = 290\times10^{-6}$ [M]

$C_{c\text{-}DE} = 0$ [M]

$C_{AQ} = 280\times10^{-6}$ [M]

I = ~9.95 [mol cm^{-2} s^{-1}] (0.15 [mW cm^{-2}])

l = 0.1 [cm]

$\varepsilon_{o\text{-}DE} = 500$ [cm^{-1} M^{-1}]

$\varepsilon_{c\text{-}DE} = 6000$ [cm^{-1} M^{-1}]

$\varepsilon_{AQ} = 2800$ [cm^{-1} M^{-1}]

$\varphi_{o\rightarrow c} = 0.46$

$\varphi_{c\rightarrow o} = 0.015$

As $\varepsilon_{o\text{-}DE}$, $\varepsilon_{o\text{-}DE}$, $\varphi_{o\rightarrow c}$, and $\varphi_{c\rightarrow o}$, the literature values in hexane were tentatively used.[2] The values of $\varepsilon_{o\text{-}DE}$ and $\varepsilon_{o\text{-}DE}$ were roughly read from the absorption spectra. The value of ε_{AQ} was roughly read from the absorption spectrum reported in our previous work.[3]

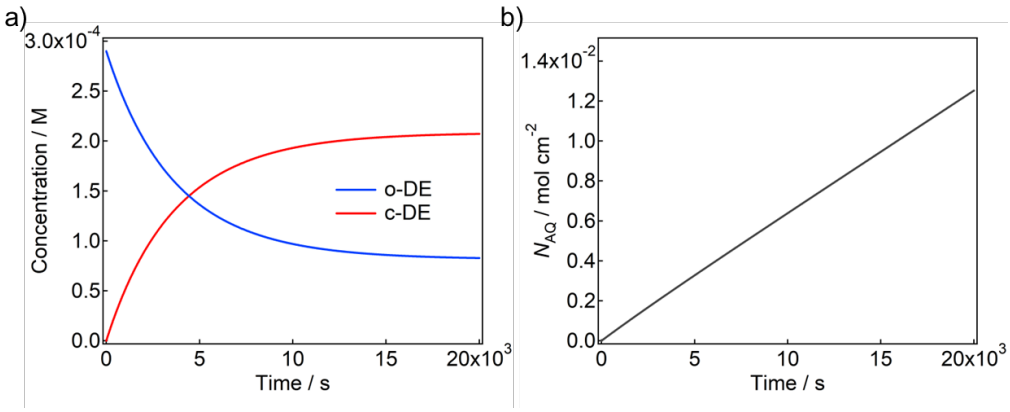

Fig. S9 Theoretical simulations of the time course of the system; (a) The concentrations of o-DE and c-DE, (b) The cumulative number of photons absorbed by AQ per area (N_{AQ}).

Multicolor photopatterning

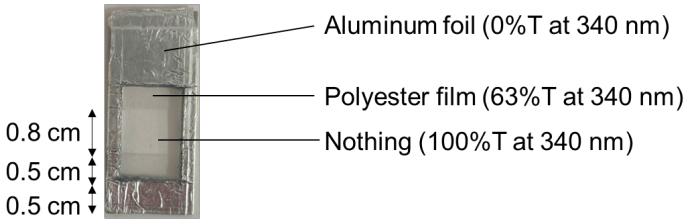

Fig. S10 An image of the photomask and its transmittance (%T) at 340 nm.

References

1 Y. Li, T. Wang and M. Liu, *Soft Matter*, 2007, **3**, 1312–1317.

2 M. Irie, K. Sakemura, M. Okinaka and K. Uchida, *J. Org. Chem.*, 1995, **60**, 8305–8309.

3 S. Fujisaki, Y. Nagai, Y. Okayasu and Y. Kobayashi, *Mater. Adv.*, 2024, **5**, 1468–1472.